Predicting load path and tensile forces during cable yarding operations on steep terrain

S. Dupire, Franck Bourrier, Frédéric Berger

Journal of Forest Research
The final publication is available at Springer via http://dx.doi.org/10.1007/s10310-015-0503-4

Predicting load path and tensile forces during cable yarding operations on steep terrain

Sylvain Dupire • Franck Bourrier • Frédéric Berger

Received: 12 August 2014 / Accepted: 26 July 2015

S. Dupire (Corresponding author)
Irstea, UR EMGR, 2 rue de la Papeterie-BP 76, F-38402 Saint-Martin-d'Hères, France
E-mail: sylvain.dupire@irstea.fr
F. Bourrier
Irstea, UR EMGR, F-38402 Saint-Martin-d'Hères, France
E-mail: franck.bourrier@irstea.fr
F. Berger
Irstea, UR EMGR, F-38402 Saint-Martin-d'Hères, France
E-mail: frederic.berger@irstea.fr

Abstract

Cable yarding systems constitute an adapted solution for steep-slope harvesting in mountain forests. However, it requires many specific skills for both forest managers and operators. The objectives of this research were to 1) develop *CableHelp* model for the set-up of cable yarding systems where inputs are operational field data and outputs are load path and tensile forces and 2) to validate it with field experiments. The results show a high accuracy between the data predicted by the model and the field measurement. Furthermore, this work stresses out the importance of taking into account both the mainline effect and the friction between skyline and intermediate supports to properly calculate the skyline tension and load path. *CableHelp* model shows a great adaptability and ensures high accuracy predictions for any positions on the line profile and for different configurations: single span or multiple span profiles, uphill or downhill yarding and for different kinds of carriage. A direct application of this research is to optimize the set-up of cable lines in order to reduce the equipment wear as well as operating cost while respecting operator safety.

Keywords Cable yarding – Load path – Cable tensile force – Cable mechanics – Steep terrain

1. Introduction

Cable yarding systems are commonly used for steep-slope harvesting in mountain areas around the world. In France, until 1960, long cables were even the only harvesting system able to reach many valleys in the Alps and Pyrenees (Bartoli 2007). Over the past fifty years, the know-how associated with this technique gradually disappeared with the heavy building of forest roads and the development of ground-based forest operation systems such as skidder (Auban and Bartoli 1997). In the others Alpine countries cable systems have persisted and have been optimized with the development of cable cranes. In Switzerland (Brändli 2010), Austria and Trento Region in Italy (Bartoli 2008), timber extracted by cable yarding represent more than 20 % of the total harvested volume. Meanwhile, in the French Alps, this figure is really lower with only 3 % of the total harvested timber (Grulois 2013). On the other hand, half of the French mountain forests are currently considered as under-harvested, partly because skidder cannot access them for technical and economic reasons (Vidal 2010). The reintroduction of cable yarding with its significant technical evolutions is an opportunity to access and manage those forests.

Set-up of the cable lines is a very technical step as well as an important part of total fixed costs of a cable yarding operation. With the growing availability of high resolution topographic datasets and the development of digital modeling, it is possible to implement decision-support tools to assess cable lines feasibility and facilitate the selection of relevant cable projects. Such a device can be composed of a Geographic Information System (GIS) based interface to locate different possible cable locations and a mechanical model to appreciate the optimal layout of intermediate supports and cable tensile forces to insure workers' safety with minimum costs.

Two different approaches are used concerning the mechanical analysis of cable yarding systems. European traditional method consists of linearized analyses of cable structures (Pestal 1961) while North American one lies on closer to reality non-linear analyses (Carson 1977; Chung 2002). Although the load path during cable yarding is a dynamic problem, all the existing methods treat it as a static case due to the relatively low speed of the load along the skyline.

The predominant cable system in Europe is known as standing skyline. The skyline is fixed to anchors at both ends implying a constant unstretched skyline length for any load weight and location. The static response to a point load by such cable structures is characterized by three main points: 1) the skyline shape and tensile forces change with the load location; 2) the cable elasticity increases the total length of the skyline and 3) the loaded span length increases by gaining some of the available unloaded adjacent spans cable length (Bont and Heinimann 2012). As shown in Lyons (2008), the cable construction stretch can be neglected when the maximum working tension is less than one-third the minimum breaking strength of the cable. This is the case in practice in the European Union where the legal safety coefficient for cable yarding systems is fixed at 3. Temperature changes can also induce an additional stretch of the skyline which is most of the time marginal and can be neglected in the calculations (Kato 1964).

In European countries, the common simplified method to assess the geometric layout of a cable road is established from linearized analyses of cable structures known as Pestal (1961) equations where only the changes in skyline shape are considered. This method lead to shorter spans and more intermediate supports than necessary as shown in previous work (Bont and Heinimann 2012).

In North America, non-linear analyses of cable structures for forestry purposes emerged with the development of computer technologies (Carson and al. 1971; Chung 1987). In this approach, cable elasticity and changes in shape and tensile forces according to load location are considered. These approaches, although more realistic, remain computer-time consuming and are concentrated on single-span cases which are not common in Europe. Bont and Heinimann (2012) developed a complete computer-aided program based on Zweifel (1960) "close-to-catenary" approach for multiple spans configuration which included all the cable responses cited previously. Their algorithm also enables optimizing the intermediate supports locations while respecting predefined safety conditions.

Although several researches in recent years related to cable systems, efforts are still needed in order to develop computerized methods that integrate accurate mathematical approaches for the structural analysis of cable systems (Cavalli 2012). This scientific lack meets the interests of forest operators and managers for an operational and accurate tool for optimizing the setup of cable yarding systems and operating this material in a safe and productive way.

Taking advantage of the previous research works, our objectives were thus 1) to develop an efficient model for the setup of cable yarding systems where inputs are operational field data such as geometric layout, initial configuration and skyline and carriage properties and outputs are the load path and tensile forces and 2) to validate this model with field experiments. The purpose of this paper is to propose an accurate forestry application of cable structure mechanics and to compare the theoretical equations used in *CableHelp* model we developed with real-world cables responses. We first focused on cable structure mechanical analysis and its adaptation to cable yarding systems. A first field experiment has then been used to validate the different model hypotheses before comparing model predictions to load path and tensile forces measured during a real cable yarding operation.

2. Model development

2.1. Available data for standing skyline

The field parameters potentially available as inputs for the design of a cable yarding system using a model were identified in close relationship with cable yarding operators. Those parameters are listed in the Table 1. The geometric layout is generally given either with the site description or by positioning the cable line on a precise Digital Terrain Model (DTM) using GIS. If a DTM is used, a raster resolution taken from 1 to 5 meters and preferably derived from ALS LiDAR data is needed for an accurate result (Akay et al. 2008). Cable and carriage properties can be given by the operators and the material manufacturers. The initial skyline tensile force has to be

The final publication is available at Springer via http://dx.doi.org/10.1007/s10310-015-0503-4

known at one of the cable ends. In practice, modern tower yarder systems generally integrate a hydraulic pressure sensor on the skyline winch. If such system is not available one can also use portable digital cable tension meter.

Table 1 *List of input parameters for the modeling of a cable yarding configuration*

Description		Abbreviation	Unit
Geometric layout	Horizontal distance between two supports	D	m
	Vertical distance between two supports	H	m
Skyline cable properties	Cable diameter	d_s	m
	Cable self-weight	q_s	$kg \cdot m^{-1}$
	Cable elasticity - Young modulus	E_s	$N \cdot m^{-1}$
	Maximum allowed tensile force	TM_s	N
Mainline cable properties	Cable self-weight	q_m	$kg \cdot m^{-1}$
	Maximum allowed tensile force	TM_m	N
Haulback cable properties	Cable self-weight	q_h	$kg \cdot m^{-1}$
	Maximum allowed tensile force	TM_h	N
Carriage property	Mass of the unloaded carriage	Q_c	kg
Load property	Mass of suspended load	Q_l	kg
Initial configuration	Carriage position on the skyline during the tensioning step (no load suspended)	s_c	m
	Tensile force measured at one of the skyline ends after tensioning step (with carriage at position s_c and no load suspended)	T_o	N

2.2. The elastic catenary: a mechanical cable structure analysis appropriated to suspended cable configuration

Figure 1 shows a cable suspended between two fixed points *A* and *B* with Cartesian coordinates (*0*,*0*) and (*D*,*H*), respectively. The span of the cable is *D*, and the vertical distance between the ends is *H*. The unstrained length of the cable L_0 corresponds to the cable length without any stress applied on it (cable self-weight is also excluded); it can also be named unstretched length. L_0 is the length that the portion of cable *AB* would have if it were laid on a totally flat terrain. A point on the cable has curvilinear abscissa *s* in the unstrained profile (the distance along the cable from the origin to that point is *s* when the cable is not stressed). When the cable self-weight force *W* is considered and a tensile force is applied at both side of the cable, the cable stretches to a new length L_u corresponding to an unloaded configuration. If, in addition to the cable self-weight force *W*, a fixed concentrated vertical load *F* is hung at a point *P* with curvilinear abscissa s_F, an additional stretch of the cable is observed and the new length of the cable is L_l. Both L_u and L_l are strained (or stretched) length of the cable and we have $L_l > L_u > L_0$.

A single cable suspended between two rigid supports can be modeled as an elastic catenary following the approach proposed in Irvine (1981). The tension within the cable *T(s)* and the Cartesian coordinates (*x(s)*, *z(s)*) of a cable point situated at curvilinear abscissa *s* are derived following a Lagrangian formulation as functions of: the unstrained length L_0, the curvilinear abscissa *s* of this cable point and, if relevant, the curvilinear abscissa s_F of the suspended load. Thereby, the shape of the cable (cable profile) is obtained by calculating all the couples of Cartesian coordinates (*x(s)*, *z(s)*) for *s* taken from 0 to L_0.

The final publication is available at Springer via http://dx.doi.org/10.1007/s10310-015-0503-4

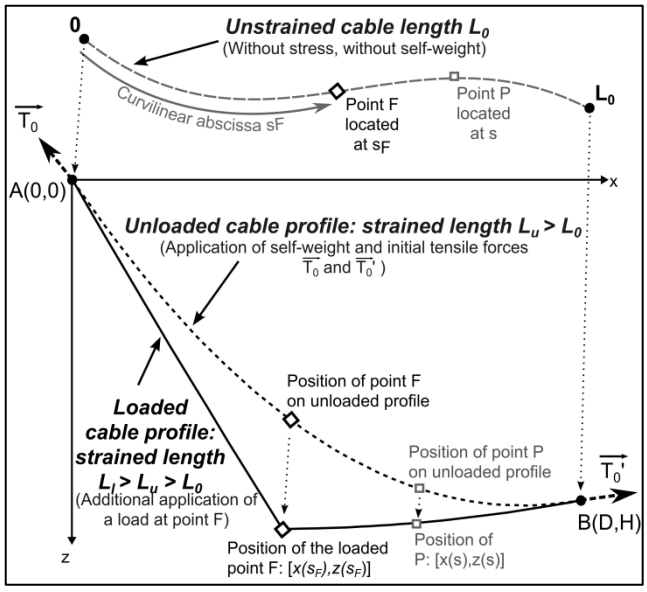

Fig. 1 Two different coordinates systems for the elastic catenary. The unstrained profile is represented in a Lagrangian frame. A point on the cable is located using the curvilinear abscissa s from the origin of the cable to this particular point. The strained profiles are represented in a two dimensional Cartesian frame (0, x, z). A point on the cable has the coordinates x(s), z(s) in the strained profiles. L0 is the unstrained cable length, Lu is the strained length of an unloaded cable and Ll is the strained length of a loaded cable.

In the case of a cable subjected only to its self-weight, the coordinates *x(s)*, *z(s)* and the tension *T(s)* in the strained cable profile are derived from Irvine (1981):

$$x(s) = \frac{T_h \cdot s}{EA_o} + \frac{T_h \cdot L_o}{W} \cdot \left[\sinh^{-1}\left(\frac{T_v}{T_h}\right) - \sinh^{-1}\left(\frac{T_v - W \cdot s/L_o}{T_h}\right)\right] \quad (1.1)$$

$$z(s) = \frac{W \cdot s}{EA_o}\left(\frac{T_v}{W} - \frac{s}{2 \cdot L_o}\right) + \frac{T_v \cdot L_o}{W} \cdot \left[\sqrt{1 + \left(\frac{T_v}{T_h}\right)^2} - \sqrt{1 + \left(\frac{T_v - W \cdot s/L_o}{T_h}\right)^2}\right] \quad (2.1)$$

$$T(s) = \sqrt{{T_h}^2 + \left(T_v - W \cdot \frac{s}{L_o}\right)^2} \quad (3.1)$$

Where:

$x(s)$	m	Horizontal cable position in the Cartesian coordinate system at curvilinear abscissa s
$z(s)$	m	Vertical cable position in the Cartesian coordinate system at curvilinear abscissa s
$T(s)$	N	Cable tension at curvilinear abscissa s
s	m	Curvilinear abscissa of a cable point
L_0	m	Unstrained cable length (initial unstretched cable length)
g	$m \cdot s^{-2}$	Constant of gravity. $g = 9.81\ m \cdot s^{-2}$
W	N	Cable self-weight force: $W = q_s \cdot g \cdot L_o$
E	$N \cdot m^{-2}$	Young's modulus (elastic modulus) of the cable
A_o	m^2	Cable uniform cross-sectional area in the unstrained profile: $A_o = \pi \cdot d_s^2/4$
T_h	N	Horizontal component of cable tension at the upper support
T_v	N	Vertical component of cable tension at the upper support

For a cable subjected to both its self-weight and a concentrated fixed load applied at s_F, the expressions of *x(s)*, *z(s)* and *T(s)* depend on the load position (s_F) and on the location of the cable point *s*. If the point is positioned

The final publication is available at Springer via http://dx.doi.org/10.1007/s10310-015-0503-4

between the upper support and the load ($0 \leq s \leq s_F$) the expressions remain similar. For a cable point situated between the load and the lower support ($s_F \leq s \leq L_0$) the expressions become (Irvine 1981):

$$x(s) = \frac{T_h \cdot s}{EA_o} + \frac{T_h \cdot L_o}{W} \cdot \begin{bmatrix} \sinh^{-1}\left(\frac{T_v}{T_h}\right) - \sinh^{-1}\left(\frac{T_v - F - W \cdot s/L_o}{T_h}\right) + \\ \sinh^{-1}\left(\frac{T_v - F - W \cdot s_F/L_o}{T_h}\right) - \sinh^{-1}\left(\frac{T_v - W \cdot s_F/L_o}{T_h}\right) \end{bmatrix} \quad (1.2)$$

$$z(s) = \frac{W \cdot s}{EA_o}\left(\frac{T_v}{W} - \frac{s}{2 \cdot L_o}\right) + \frac{T_h \cdot L_o}{W} \cdot \begin{bmatrix} \sqrt{1 + \left(\frac{T_v}{T_h}\right)^2} - \sqrt{1 + \left(\frac{T_v - F - W \cdot s/L_o}{T_h}\right)^2} + \\ \frac{F \cdot W}{T_h \cdot EA_o}\left(\frac{s_F}{L_o} - \frac{s}{L_o}\right) + \sqrt{1 + \left(\frac{T_v - F - W \cdot s_F/L_o}{T_h}\right)^2} - \sqrt{1 + \left(\frac{T_v - W \cdot s_F/L_o}{T_h}\right)^2} \end{bmatrix} \quad (2.2)$$

$$T(s) = \sqrt{{T_h}^2 + \left(T_v - F - W \cdot \frac{s}{L_o}\right)^2} \quad (3.2)$$

Where:

s_F	m	Curvilinear abscissa of the load location on the unstrained cable profile
F	N	Concentrated vertical load applied at the curvilinear abscissa s_F.

F depends on the carriage Q_c and load Q_l weights and on the self-weights of the mainline q_m and of the haulback line q_h: $F = g \cdot \left[Q_l + Q_c + \frac{1}{2}(s_F \cdot q_m + (L_o - s_F) \cdot q_h)\right]$

These expressions contain as unknowns the horizontal (T_h) and vertical (T_v) reactions of the supports at the origin A. These quantities can be determined by solving the two dimensional system of equations $\begin{cases}(1.2)\\(2.2)\end{cases}$. The resolution of this system allows calculating the quantities required for the design of a cable yarding system. Amongst them, we are particularly interested in the load path (i.e. the sequence of load positions taken from 0 to L_0) and the evolution of the maximum tensile force $T(s=0)$ according to the load position. In practice, knowing the position of the load allows ensuring that it does not touch the ground or that a minimum clearance between the load and the ground is respected. The accurate estimation of the maximum tensile force of the skyline for a given configuration enables checking the safety condition of the operators. This method also enables calculating the shape of the cable for each load position for the loaded profile.

2.3. Adaptation of the elastic catenary to a standing skyline configuration

2.3.1. General model structure

The approach proposed in Irvine (1981) has been adapted to account for standing skyline specificities. The main assumption governing our model is that the unstrained (or unstretched) skyline length L_0 for the entire profile remains the same whatever the carriage position s_F or load force F is. On the other hand, the strained (or stretched) skyline length L is evolving according to both the carriage configuration (loaded or unloaded) and its position s_F along the cable profile. The second hypothesis is that the magnitude of the skyline tensile force evolves continuously along the cable profile except from three situations: 1) at intermediate supports level (only for multiple span configurations), 2) if the carriage is locked to the skyline or 3) if the carriage is self-motorized. In the first point, the friction between the skyline and the jack modifies the tensile force so that the tension measured at the loaded span

side is higher than the one at the unloaded span side. In the two last points the skyline tensile force at the upper side of the carriage is higher than the one at lower side as explained in Irvine (1981).

Taking into consideration these assumptions, the general process of the model follows two main steps: 1) Using the two-dimensional equations system $\begin{cases}(1.2)\\(2.2)\end{cases}$ and the appropriate initial settings, search of the initial unstrained length of the skyline for the entire profile L_0 which corresponds to the tension T_0 measured on the field for an unloaded carriage at position s_c and 2) calculation of the load path and tensile forces within the skyline for different load positions s_F along the cable taken from 0 to L_0. According to the configuration tested and the type of carriage used for the operation, an additional step may be needed and consists in estimating the mainline or haulback influence and the friction between the skyline and the jack at intermediate supports.

The first step of the process is to calculate the unstrained skyline length L_0 from the initial settings of the system. An important point in our model is to use operational data as inputs. In order to meet the same initial conditions as observed on the field, the model calculate the unstrained cable length L_0 corresponding to the skyline tensile force T_0 measured at one of the cable ends during the tensioning step and with an unloaded carriage located at curvilinear abscissa s_c. L_0 is initially fixed as the shortest distance between both supports (i.e. the diagonal distance) corrected with the cable elasticity:

(4) $$L_0(initial) = \sqrt{D^2 + H^2} \Big/ \left(1 + \frac{4 \cdot T_0}{E \cdot \pi \cdot d^2}\right)$$

An iterative method is then used to find L_0. The skyline tension $T(s)$ at the same support where T_0 was measured is calculated using the following boundary conditions in the two-dimensional system of equations $\begin{cases}(1.2)\\(2.2)\end{cases}$: $s = L_0$, $x(s) = D$, $z(s) = H$, $s_F = s_c$. While $T(s)$ is significantly different than T_0 (by default $|T(s) - T_0| \leq 10$ N), L_0 is incremented with a small length δ (by default $\delta = 0.001$ m). For each new iteration, a two-dimensional Newton-Raphson's method (Ypma 1995) is used to find the unique solution (T_h, T_v) of the system of equations $\begin{cases}(1.2)\\(2.2)\end{cases}$ that allows calculating $T(s)$.

The second step of the process is to calculate the load path and the maximum skyline tensile force on the loaded span. Once the unstrained cable length L_0 is known, the full load (i.e. loaded carriage) is applied and the model automatically moves the load each meter along the unstrained profile from the upper support ($s_F = 0$) to the lower support ($s_F = L_0$). For each load position s_F, the couple (T_h, T_v) solution of the system of equations $\begin{cases}(1.2)\\(2.2)\end{cases}$ is determined and used to calculate the load position ($x(s_F)$,$z(s_F)$) and the theoretical maximum skyline tension $T(s=0)$. This quantities are calculated with the equations *(1.2)* for $x(s_F)$, *(2.2)* for $z(s_F)$ and *(3.1)* for $T(s=0)$. At the end of this process, all the load positions obtained represent the trajectory of the load. Moreover, the evolution of the maximum skyline tension $T(s=0)(s_F)$ according to the load location is generated.

2.3.2. Calculation of the skyline tensile force with a configuration using a mainline

The method exposed in Irvine (1981) deals with a fixed point loaded on the cable. This is true when considering either a self-motorized carriage or when the carriage is locked on the skyline (during loading and unloading phases).

As shown in Figure 2a, considering a fixed load implies that the magnitudes of skyline tension at each side of the carriage are not equal. The magnitude at upper side of the carriage T_{1l} is equal to $T(s=s_F)$ in equation (*3.1*) while the magnitude at the lower side of the carriage T_{2l} is equal to $T(s=s_F)$ in equation (*3.2*). As a consequence, in this configuration T_{1l} is always greater than T_{2l} (Irvine 1981).

The final publication is available at Springer via http://dx.doi.org/10.1007/s10310-015-0503-4

However, during cable yarding operations, the load may move on the skyline with the help of one (uphill yarding) or two (downhill yarding) cable(s). Figure 2b shows the same case as Figure 2a but with the carriage hold by the mainline and not locked on skyline. With this configuration the skyline is free to move at the carriage level, the magnitudes of the tension at each side of the carriage are consequently equal ($T_{1f} = T_{2f}$) and the mainline (or haulback) tensile force $\overrightarrow{T_m}$ required to hold the carriage contributes to support the concentrated load $\vec{F}$.

The assumption made to solve this situation is that the Cartesian coordinates of the carriage ($x(s_F)$,$z(s_F)$) when the carriage is hold with a mainline is not significantly different from the coordinates when the carriage is locked on the skyline. The mainline tension is estimated from the equilibrium equations of the carriage as shown in Figure 2b. The angles α (between the left side of the skyline and the horizontal) and β (between the right side of the skyline and the horizontal) can be calculated as shown in equation (5) where ε is a small distance representing the vicinity of the carriage. λ is the angle between the horizontal and the mainline.

$$(5) \qquad \alpha = \sin^{-1}\left|\frac{z(s_F-\varepsilon)-z(s_F)}{\varepsilon}\right|, \quad \beta = \sin^{-1}\left|\frac{z(s_F+\varepsilon)-z(s_F)}{\varepsilon}\right|$$

The equilibrium equations of the carriage lead to the expression of the mainline tensile force T_m (equation *(6)*) and of the skyline tensile force at both side of the carriage T_{1f} and T_{2f} (equation *(7)*).

$$(6) \qquad T_m = F \cdot \frac{\cos(\beta) - \cos(\alpha)}{\sin(\alpha-\lambda) + \sin(\lambda+k\cdot\beta)}$$

$$(7) \qquad T_{1f} = T_{2f} = F \cdot \frac{\cos(\lambda)}{\sin(\alpha-\lambda) + \sin(\lambda+k\cdot\beta)}$$

Where k = 1 if $\overrightarrow{T_{2f}}$ is oriented upwards and k = -1 if $\overrightarrow{T_{2f}}$ is oriented downwards

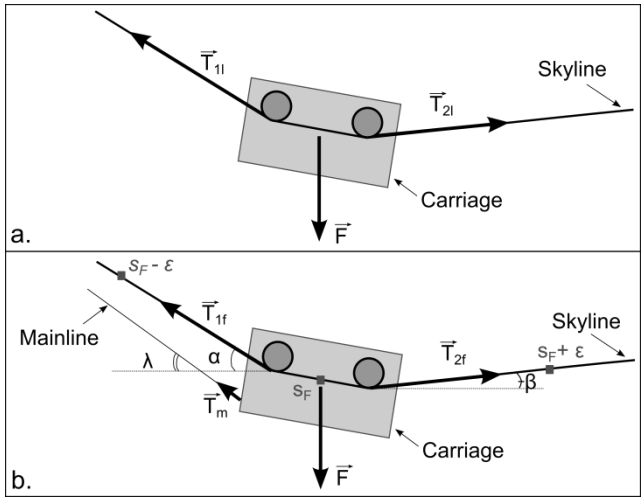

Fig. 2 *Forces acting in the equilibrium equation of the carriage. When the carriage is locked on the skyline or is self-motorized (a) the magnitude of the skyline tension at the upper side of the carriage T_{1l} is greater than magnitude at the lower side of the carriage T_{2l}. When the carriage is hold by the mainline (b) at curvilinear abscissa s_F, the magnitudes of the skyline tension at both sides of the carriage are considered as equal ($T_{1f} = T_{2f}$).*

This calculation process has to be repeated for each new load location s_F. When using a horizontal symmetry, this method can also be applied to downhill yarding. At the end, the skyline tensile force taking into consideration the mainline influence is calculated for any point s_F along the unstrained cable length.

The final publication is available at Springer via http://dx.doi.org/10.1007/s10310-015-0503-4

2.3.3. Multiple span configurations and skyline friction at intermediate supports

Additional calculation steps have to be added to account for multiple span configurations, especially for the calculation of the initial layout and for modeling the displacement of the skyline according to the load position.

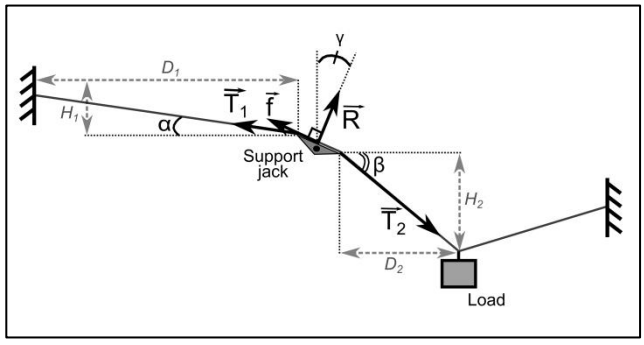

Fig. 3 *Calculation of skyline friction at intermediate support*

A friction force $\vec{f}$ at intermediate supports between the skyline and the jack may additionally be taken into account when considering a multiple span configuration (see Figure 3). The direction of the support reaction force $\vec{R}$ is assumed to be along the bisectrix between both sides of the skyline. The angle γ between $\vec{R}$ and the vertical can be taken conveniently as $\gamma = \frac{(\beta+\alpha)}{2}$. The friction force $\vec{f}$ is oriented in the opposite direction compared to $\vec{T}_2$ as the skyline moves from the unloaded span to the loaded span. A classical Coulomb friction model is used to relate *f* and *R* as shown in equation *(8)* where the friction angle φ depends on the materials on which the friction takes place.

(8) $$f = R \cdot \tan\varphi$$

Considering the equilibrium equation of the skyline portion lying on the jack, it is possible to obtain the skyline tensile force at the unloaded span side T_1 and the support reaction force R:

(9) $$T_1 = T_2 \cdot \frac{\cos(\beta-\gamma)+\sin(\gamma-\beta)\cdot\tan\varphi}{\cos(\alpha-\gamma)+\sin(\gamma-\alpha)\cdot\tan\varphi} \quad \text{and} \quad R = T_2 \cdot \frac{\sin(\beta-\alpha)}{\cos(\alpha-\gamma)+\sin(\gamma-\alpha)\cdot\tan\varphi}$$

The process presented above for accounting for the friction force is used during the two main phases of the multiple span modeling. As for single span, the first phase consists in estimating the total unstrained cable length L_0 on the entire profile. A step by step process is used to find L_0. We first process span 1 noted *S1* where the initial skyline tension T_0 and the unloaded carriage position s_c are known. The unstrained skyline length L_{0_S1} is calculated following the same process as for single span. Once L_{0_S1} is known, it is possible to calculate the skyline tensile force T_{01} at the first intermediate support *IS1*. This tensile force is corrected taking into account the friction force at intermediate support *IS1* to give T_{01f} the tensile force at the upper side of span 2. Second, the unstrained cable length L_{0_S2} for the span 2 is handled similarly by replacing T_0 by T_{01f} and s_C by 0. We obtain T_{02} at the second intermediate support *IS2* which is corrected taking into account the friction at intermediate support to give T_{02f}. The same process is used for the *n* spans *Si* of the multiple span configuration. Finally the total unstrained cable length L_0 is obtained by summing all the individual span lengths:

(10) $$L_0 = \sum_{i=1}^{n} L_{0\_Si}$$

The final publication is available at Springer via http://dx.doi.org/10.1007/s10310-015-0503-4

The second phase consists in calculating the load path and maximum skyline tensile force along the entire profile. For a standing skyline configuration the total unstrained cable length L_0 that corresponds to the initial settings has to remain constant no matter if the skyline is loaded or unloaded. The total unstrained skyline length L_{0_l} in loaded configuration is calculated following the equation *(11)*:

(11) For a load located on span *i*: $$L_{0\_l} = L_{0\_lS} + \sum_{j=1}^{j=i-1} L_{0_{lSj}} + \sum_{j=i+1}^{j=n} L_{0_{lSj}}$$

In equation *(11)*, L_{0_lS} corresponds to the unstrained length of the skyline on the loaded span *i* and L_{0_lSj} corresponds to the unstrained length of the skyline on the other spans *j* (with $j \neq i$). An iterative method is used to find the correct L_{0_lS} that induces $L_{0\_l} = L_0$.

A step by step process is used where L_{0_lS} is initially taken as equal to L_{0_Si}. Knowing L_0, the skyline tensile forces T_{i-1} and T_i at both ends of the loaded span can be calculated. These forces are corrected with the friction force to give respectively T_{i-1f} and T_{if}. The unstrained skyline lengths L_{0_lSi-1} and L_{0_lSi+1} of the adjacent unloaded spans are then calculated by seeking the value that match the tensile force known at the end they have in common with the loaded span. The *n* spans of the profile are processed step by step in order to ensure that the magnitude of the tensile force is evolving continuously along the profile. Finally we obtain the total unstrained skyline length for a loaded configuration L_{0_l}.

For each load position s_F, the model iterates on the unstrained skyline length L_{0_lS} of the loaded span. When the total unstrained skyline length for a loaded configuration L_{0_l} corresponds to the initial total unstrained skyline length L_0 (by default the tolerance is $| L_{0_l} - L_0 | \leq 0.001$m), the process stops and the load position and maximum tensile force are calculated.

This process allows respecting the two main assumptions of a constant unstrained length and of a magnitude of the skyline tensile force evolving continuously along the profile (including the exceptions raised before concerning that point). All the calculation process has been computed in the *CableHelp* model using the open source Python language with its associated libraries Numpy (Oliphant 2007) and Matplotlib (Hunter 2007).

3. Field experiments

Field experiments were set up with the aim of comparing field results with model predictions in terms of skyline tensile force and cable profiles for different load positions along the cable. Accurate comparison requires specific and precise measurements of the cable positions and tensile forces that cannot be carried out easily during real cable yarding operations without disturbing it. Moreover, it is practically complex to design small-scale experiments fulfilling similitudes rules. These reasons lead us to build a first standing skyline system with the objectives of validating our assumptions and getting first elements of the model relevance. This experiment has been completed with measurements done during a real cable yarding operation.

3.1. Single and double span experiments

A first set of configurations has been carried out in the park in front of the center Irstea – Grenoble (experimental set up see Annex 2). 7 single span and 3 double span configurations have been tested. Their characteristics are described in Table 2. First, the trees (DBH 40 to 45 cm) serving as supports have been anchored to ensure their stability. A load cell has been installed on the first tree and plugged to a data logger. One side of the skyline has

The final publication is available at Springer via http://dx.doi.org/10.1007/s10310-015-0503-4

been fixed directly on the load cell and the other to a manual hoist used to stretch it. Reference points have been previously marked each meter along the unstrained skyline with origin at the cable end situated at the load cell level. The carriage movement was ensured by the mainline or the haulback according to its position. Those cables were moving with the help of manual hoists. The load was represented by a 265 kg steel ball lifted up with an electric hoist (75 kg) tied on the carriage (25 kg). For the 3 double span configurations, a load cell has also been added on the upper side of the carriage to measure the mainline tension. For each configuration tested, the load was positioned successively on each point of reference previously marked on the skyline (i.e. each meter in the curvilinear unstrained cable profile). For each load location we measured: the tensile force in the skyline and three pairs of coordinates *(x, z)* for the positions of the carriage and both cable ends. These coordinates were measured using a total station combining an electronic theodolite with an electronic distance meter.

Table 2 *List and description of field experiments followed up*

Code	Configuration	Load cell location	Span 1		Span 2		Span 3		Initial settings		Skyline properties		
			D_1 m	H_1 m	D_2 m	H_2 m	D_3 m	H_3 m	T_0 N	F N	d_s mm	E_s kN·mm^{-2}	q_s kg·m^{-1}
L-U	Single span	Lower support	15.0	0.3					770	1015	16.2	100	1.02
L-L	Single span	Lower support	14.9	0.3					770	3595	16.2	100	1.02
U1_U	Single span	Upper support	14.9	1.9					780	925	16.2	100	1.02
U1_L	Single span	Upper support	14.9	1.9					780	3505	16.2	100	1.02
U2_L	Single span	Upper support	14.8	1.9					1200	3505	16.2	100	1.02
U3-U	Single span	Upper support	14.9	2.0					900	925	16.2	100	1.02
U3-L	Single span	Upper support	14.87	1.9					900	3505	16.2	100	1.02
Do1	Double span	Upper support	15.3	2.3	20.3	1.2			380	3540	16.2	100	1.02
Do2	Double span	Upper support	15.4	2.2	20.3	1.1			290	3540	16.2	100	1.02
Do3	Double span	Upper support	15.3	2.4	20.3	1.4			290	3540	16.2	100	1.02
RCYO	Real operation	Anchorage	24.1	14.78	197.4	113.0	39.7	24.8	45000	14024	16.0	91	1.23

3.2. Real cable yarding operation

The first experiment presented the advantage of being relatively easy to implement but it has three major disadvantages. First, the spans were short comparing to the skyline characteristics (d_s, q_s, E_s). This may produce a system that is insensitive to elasticity and self-weight of the cable. Second, the skyline slope in the single and double span experiments varies from 2 % to 14 % which correspond to relatively flat configurations. During real cable yarding operations the skyline slope is often larger than 40 %. Third, the trees used as anchor might represent more rigid supports than in real cable yarding operation as the skyline tension applied was small comparing to real configurations.

These three main disadvantages lead us to follow a real cable crane operation in the National forest of Gargas situated in a northern slope of the French Alps (UTM Long 5°55'17", Lat 44°52'37", see Annex 3). The cable yarding operation was ensured by a small cable crane (Larix Lamako) with an uphill extraction of the logs. The carriage (Sherpa U 3T) moved with the help of both a mainline and a haulback line ($q_m = q_h = 0.529$ kg·m^{-1}). Only one intermediate support was present and placed at the upper part of the profile. The total horizontal length of the profile was about 260 meters and the vertical length of about 150 meters. The average chord slope of the spans is about 60%. The total suspended weight is of 1 430 kg (Q_c = 410 kg and Q_l = 1020 kg). The last configuration *RCYO* of the Table 2 gives details of this configuration.

The final publication is available at Springer via http://dx.doi.org/10.1007/s10310-015-0503-4

The skyline tensile force was measured with a 20 kN load cell located at the anchor level to avoid damaging the skyline. The load path was measured with a total station associated to its specific target which was previously fixed on the carriage. The measurements concern 30 static positions only located on the second span (the longest one). The carriage was hold with the mainline and the load was fully suspended. For each position we waited for the equilibrium of the carriage before measuring the skyline tensile force and the position of the carriage.

4. Results : Comparison between field experiments and model prediction

4.1. Single and double span experiments

4.1.1. Load path

As described above, we considered that the load path is not affected by the eventual corrections induced by the mainline or the friction at intermediate support. 123 positions gathering all the single and double span configurations have been measured during the field experiments. All of them have been taken into account in the load path comparison. The load path is calculated respectively with equation *(1.2)* for the *x* axis and equation *(2.2)* for the *z* axis. Table 3 shows the root-mean-squared error (RMSE), the coefficient of variation of the root-mean-squared error CV(RMSE) and the bias between the measured and predicted load path along both *x* and *z* axis for the 10 different configurations tested. The model predicted the load path along *x* axis with a RMSE from 0.1 to 3.6 mm. The error along *z* axis is higher with a RMSE from 0.3 to 7.5 mm. For both *x* and *z* axis, the coefficient of variation of the RMSE is nearby 0 % and no systematic bias is observed.

Table 3 *Comparison between load path experimental measurements and data predicted by CableHelp model for the 10 different configurations tested (single and double span included) during the single and double span field experiments*

Configuration	Number of observations	Load path on the *x* axis			Load path on the *z* axis		
		RMSE mm	CV(RMSE) %	Bias mm	RMSE mm	CV(RMSE) %	Bias mm
1 span L – U	15	2.1	0.03	-0.3	3.7	0.07	3.1
1 span L – L	14	0.2	0.00	0.0	0.3	0.01	0.2
1 span U1 – U	7	2.0	0.03	0.4	4.0	0.09	3.3
1 span U1 – L	14	0.2	0.00	0.1	0.4	0.01	-0.1
1 span U2 – L	14	0.1	0.00	0.0	0.3	0.01	-0.2
1 span U3 – U	4	0.7	0.01	0.0	2.5	0.05	2.1
1 span U3 – L	14	0.1	0.00	0.0	0.4	0.01	-0.2
2 spans Do1	24	0.1	0.00	0.0	0.7	0.02	-0.6
2 spans Do2	5	3.6	0.07	0.2	7.5	0.15	-1.4
2 spans Do3	13	0.1	0.00	-0.1	1.1	0.04	-1.0
All observations	124	1.1	0.02	/	2.3	0.05	/

4.1.2. Tensile forces

Figure 4 shows the effect of the correction of mainline tension on the skyline tensile force for the single span configuration U2–L. In this configuration, the cable profile was inclined and the load cell was placed at the upper support with curvilinear abscissa 0. Without correction, the skyline tension prediction is higher than the field

The final publication is available at Springer via http://dx.doi.org/10.1007/s10310-015-0503-4

measurements when the load is close to the upper support; it comes closer to the field measurements when the load position is situated nearby the basal point of the cable profile. The correction proposed for the skyline tensile force prediction improves the accuracy.

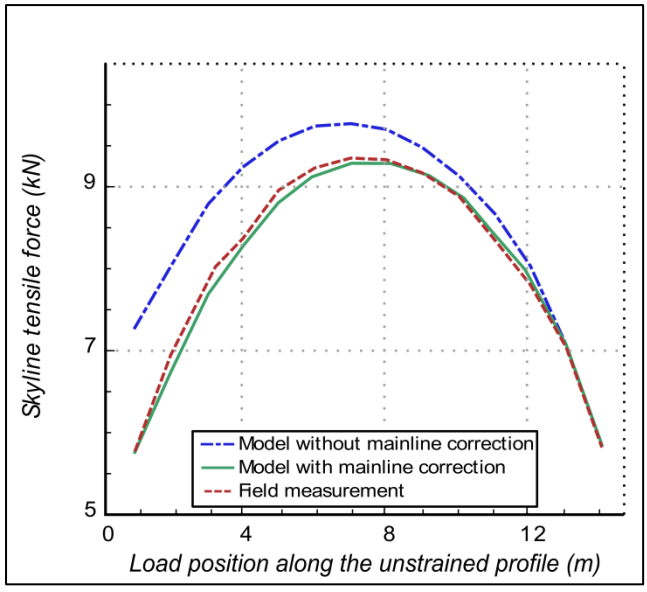

Fig. 4 *Comparison of skyline tensile force measured on field with the data predicted using the model with and without mainline tension correction for the configuration U2 - L. Corrected model prediction better fits the field measurement*

Table 4 presents the RMSE, CV(RMSE) and bias observed for the 7 different single span configurations tested. As noticed in Figure 4, the correction of the skyline tension with the mainline tension induces a positive effect. The error and the coefficient of variation are divided by a factor 3.6. After correction, the error concerning the skyline tension is between 64 and 199 N and the average coefficient of variation is 2.7 %.

Table 4 *Comparison between experimental measurements of tensile forces and data predicted by CableHelp model for the 7 different single span configurations tested*

Configuration	Number of observations	Skyline Tension without correction			Skyline Tension corrected		
		RMSE N	CV(RMSE) %	Bias N	RMSE N	CV(RMSE) %	Bias N
1 span L – U	15	74	3.31	15	64	2.94	-22
1 span L – L	14	401	6.33	218	160	2.66	-120
1 span U1 – U	7	180	7.97	158	70	3.34	4
1 span U1 – L	14	816	11.96	702	140	2.28	33
1 span U2 – L	14	654	7.75	570	199	2.55	-77
1 span U3 – U	4	64	1.86	62	97	2.94	-55
1 span U3 – L	14	663	7.71	530	193	2.44	-128
All observations	82	541	9.74	/	150	2.70	/

The mainline tension has been measured only for the 3 double span configurations for a total of 42 positions. The comparison between field measurements and predicted values gives an average error of about 76 N, a coefficient of variation of about 12 % and a bias of – 30 N. Figure 5 shows the linear regression between the measurements carried out during the field experiment and the model predictions. The model predictions concerning

The final publication is available at Springer via http://dx.doi.org/10.1007/s10310-015-0503-4

the mainline tension are rather scattered around the regression line (R^2 = 0.984). The skyline tension is better predicted with less dispersion around the regression line (R^2 = 0.997).

Fig. 5 *Comparison between experimental field measurements (abscissa) and data predicted by the model (ordinate). The mainline tension and the corrected skyline tensile force are shown respectively in (**a**) and (**b**). 42 positions are considered for the mainline tension and 82 for the skyline tension*

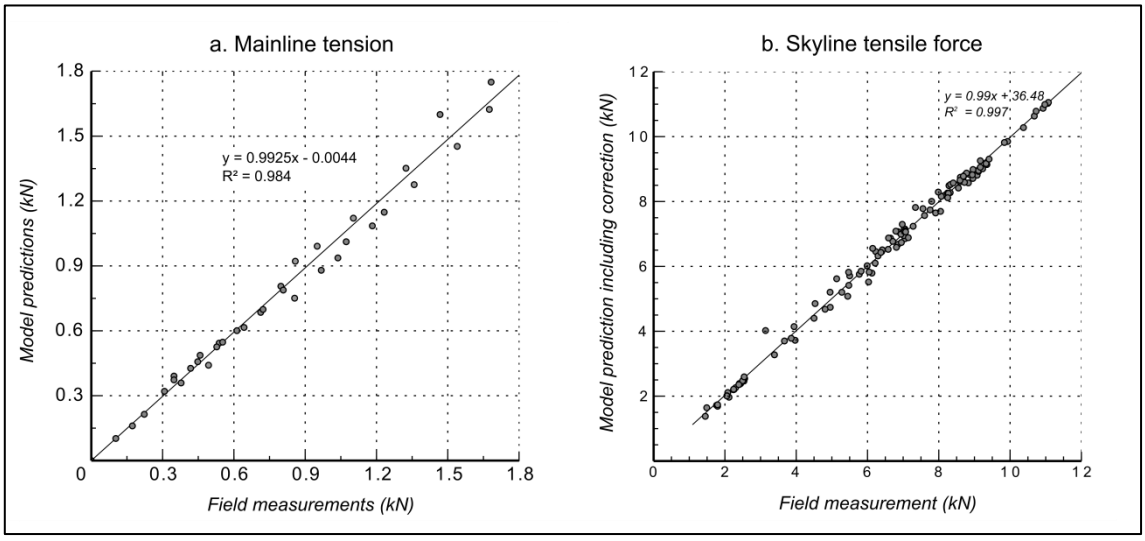

4.1.3. Double span and skyline friction at intermediate support

For the three double span configurations tested, the skyline tension was measured at the upper extremity on the first span. Therefore, when the load is located on the second span it is possible to analyze the influence of the friction between the skyline and the intermediate support. Table 5 shows the influence of the friction angle value on the skyline tension predicted by the model (with mainline correction). If no friction is considered (friction angle is 0 rad), a systematic positive bias is observed. On the contrary, when the friction angle is high (0.3 rad), the model predicts lower tension values than measured during the field experiment (about –470 N). With a friction angle equal to 0.15 rad the skyline tension predicted by the model is very close to the one measured during the field experiments as shown with Figure 6.

Table 5 *Example of the influence of the friction angle value on the skyline tension predicted by CableHelp model for the configuration Do2*

Friction angle	Skyline Tension		
	RMSE	CV(RMSE)	Bias
rad	N	%	N
0 (no friction)	465	6.38	394
0.1	151	2.07	98
0.15	107	1.47	-46
0.2	226	3.10	-186
0.3	526	7.22	-468

Table 6 shows the RMSE, CV(RMSE) and bias observed concerning the skyline tensile force after correction of the mainline tension and with a friction angle of 0.15 rad. The model predicts as accurately the skyline tensile forces

The final publication is available at Springer via http://dx.doi.org/10.1007/s10310-015-0503-4

for double span as for single span with a RMSE of about 205 N. The coefficient of variation is similar than for single span and no systematical bias is observed.

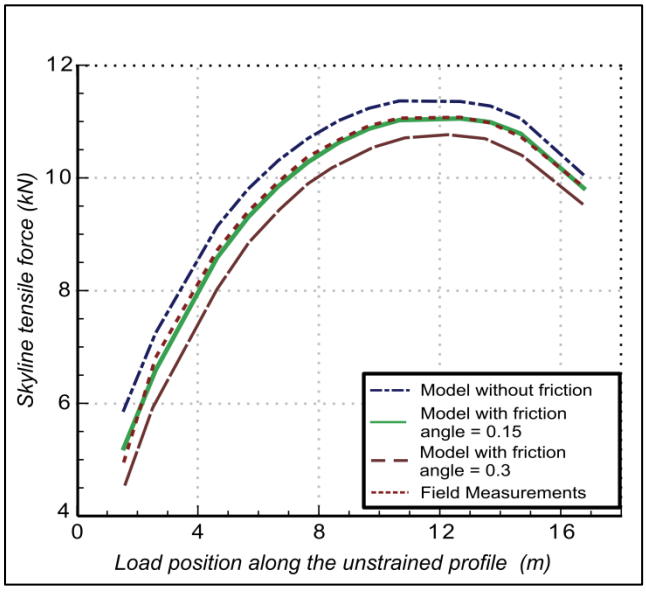

Fig. 6 *Influence of the friction of the skyline with the intermediate support on the skyline tension predicted by the model for the configuration Do2. If no friction is taken into account, the predicted tension is systematically above the measured tension. With a friction angle of 0.15 rad, experimental curve fits the modeling curve. Finally, with a friction angle of 0.3 rad, model predictions are above the experimental values*

Table 6 *Comparison between experimental measurements of tensile forces and data predicted by CableHelp model for the 3 different double span configurations tested. The correction takes into account the mainline tension and a friction angle of 0.15 rad*

Configuration	Number of observations	Skyline Tension corrected		
		RMSE N	CV(RMSE) %	Bias N
2 spans Do1	24	211	2.85	75
2 spans Do2	5	160	2.09	54
2 spans Do3	13	208	2.15	-154
All observations	42	205	2.52	/

4.2. Real cable yarding operation

30 observations have been measured during the follow up of the real cable yarding operation. These data are compared with the outputs of the model in Table 7. Four modeling options have been considered: 1) model integrating mainline and friction effect, 2) model considering only mainline effect, 3) model considering only friction effect and 4) strict application of the model without any correction concerning mainline or friction.

Table 7 shows the RMSE, CV(RMSE) and bias observed for the load path and skyline tensile force for each option. The load path is best predicted with the option integrating mainline effect and friction at intermediate support. The model integrating mainline alone or friction alone improve also the prediction observed with the basic option without any correction.

The final publication is available at Springer via http://dx.doi.org/10.1007/s10310-015-0503-4

Table 7 *Comparison between the 30 cable yarding field measurements and model prediction according to different options for the modeling*

Model parameters	Load path on the *x* axis			Load path on the *z* axis			Skyline Tension		
	RMSE	CV (RMSE)	Bias	RMSE	CV (RMSE)	Bias	RMSE	CV (RMSE)	Bias
	m	%	m	m	%	m	N	%	N
Mainline + friction	0.081	0.08	0.056	0.146	0.21	0.129	1135	1.56	651
Mainline only	0.149	0.14	0.138	0.240	0.24	0.233	1050	1.43	909
Friction only	0.191	0.18	-0.145	0.332	0.48	-0.266	2655	3.72	-929
No correction	0.275	0.26	-0.239	0.442	0.64	-0.384	2387	3.35	-1038

The skyline tension is best predicted with the models integrating the mainline effect. As shown in Figure 7, the shape of the two curves corresponding to the two options with mainline fit the field measurements curve. For these two options the RMSE is about 1.1 kN and the coefficient of variation is about 1.5%. The curves corresponding to the model without mainline correction are lower than the field experiment curve at the lower part of the profile. For these options the RMSE is about 2.5 kN and the coefficient of variation about 3.5%.

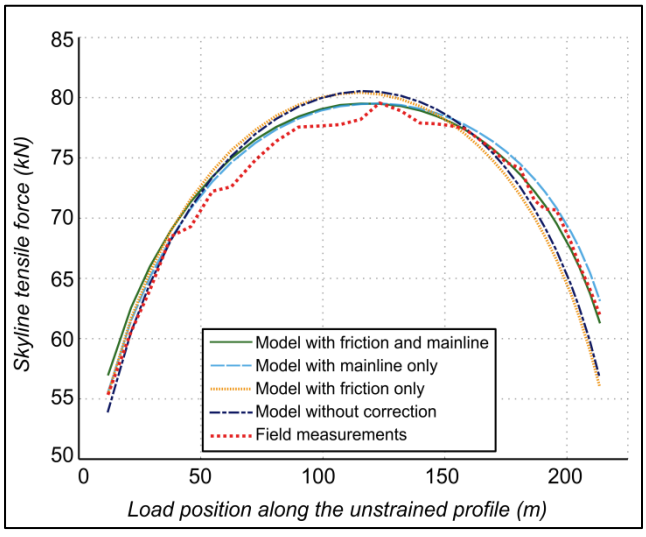

Fig. 7 *Comparison between skyline tensions predicted by the model and the 30 field measurements according to different options for the modeling.*

The mainline integration influences the bias observed as it is positive for all variables when mainline is considered and negative when it is not considered. Integrating the friction has a positive effect on the load path prediction and a slight negative effect on the skyline tension prediction.

Finally, to appreciate the importance of skyline elasticity in the model, a "rigid" cable has been modeled (E-modulus was changed from 91 to 310 $kN \cdot mm^{-2}$). With the rigid cable, the basic application of the model (no correction of mainline and friction effect) returns less accurate predictions. Thus, the errors on load path and skyline tensile force increase respectively by a factor 1.5 (about 0.7 m) and 3.3 (about 8000 N) comparing to the basic application of the model with the real skyline elasticity.

The final publication is available at Springer via http://dx.doi.org/10.1007/s10310-015-0503-4

5. Discussion and conclusion

Our research was aimed at 1) developing a numerical application for the setup up of cable yarding systems that uses operational field data as inputs and returns load path and tensile forces as outputs and 2) validating the method and the results with field measurements.

This research produced the following major findings. First, the approach proposed is closely related to the practical use of operational field data, especially when modeling the initial settings of a particular configuration. In most of the previous approaches, the basic tensile force T_0 corresponds to the initial tension without a carriage mounted on the skyline which in practice is not the case. As far as we know, the method proposed in this paper is the first to consider the carriage during this tensioning step when modeling the initial settings. The weight of the carriage alone can represent between 10 % and 25 % of the total suspended weight during the yarding step. Therefore, neglect the carriage weight when modeling the initial settings leads systematically to predict higher skyline tensile force when a load is applied.

Second, our study shows that the elastic catenary solution proposed in Irvine (1981) and the adaptation performed within this work is appropriate to predict with a high accuracy the load path and tensile forces during cable yarding operations. The comparison between the experiments and the outputs of the model showed a high accuracy in the load path prediction. For the real experiment the error varies from 17 cm (0.07 %) for a complete application of the model (with mainline and friction) to 52 cm (0.23 %) for a basic application of the model (no friction, no mainline). Accuracy concerning the position of the load allows ensuring that it does not touch the ground or that a minimum clearance between the load and the ground is respected. This method has the same range of error as average precision (2 points·m^{-2}) DTM in mountainous regions built from airborne laser scanning (Hollaus and al. 2006). The model can therefore be used together with this kind of DTM to optimize the mounting of the line and the position of intermediate supports.

Skyline tension is also predicted with good accuracy with a maximum error of 2 655 N (3.7 %) in real conditions. In practice, tensile force is usually only checked during the setting of the line, the maximum loaded skyline tension is estimated based on the experience of operators and supposed to reach the safety recommendations. Our model allows precisely assessing this parameter taking into account the initial layout and enables checking the safety of operators. The wear of the material in loaded configuration can also be minimized as the minimal initial tensions needed for a correct functioning of the system can be also calculated.

The method proposed to estimate mainline tension shows a larger error (from 6 to 12 % in the first experiment). However, our results in the experimental configurations as well as in the real configuration show the importance of taking into account the mainline to predict accurately the skyline tension. Our approach could be certainly improved taking into account the interval between the two opposite wheels of the carriage in order to better transcribe its inclination. Potential improvements of both field measurements and model assumptions can also be envisaged to reduce the observed error of the mainline tension.

Third, our work stresses the influence of the friction between the skyline and the intermediate support. Most of the previous works (Charland and al. 1994; Chung and Sessions 2003; Bont and Heinimann 2012) considers that the friction between the rope and the jack can be neglected. However, our study shows its effect on skyline tension and load path. The study carried out by McColl and al. (1995) demonstrated that, for a contact between a lubricated steel rope (skyline) and a steel surface (support jack), the friction angle can conveniently be taken in a range from 0.1 to 0.2 rad. The best prediction of skyline tension is obtained using a friction angle of 0.15 rad which is the median value of this range.

Fourth, to our knowledge, the complete experimental follow up of load path and tensile forces (in both skyline and mainline) for cable yarding configurations done within this study constitutes an exhaustive data set for the complete assessment of cable yarding systems design and for the evolution of their modeling. Among the previous

researches, Sessions (1976) provided a method for estimating skyline tension and avoiding overload. Fabiano and al. (2011) followed the skyline tension with load cells for 69 cable lines and provided an interesting sum up of these field measurements. However, none of these works linked precisely skyline tension with load path.

More generally, this approach takes into account the three main points describing the cable response to a point load: changes in skyline shape and tensile forces according to the load position, changes of cable length due to cable elastic stretch and the multiple span specificities. Moreover, the model proposed demonstrates a high adaptability to many terrain configurations. Load path and tensile forces can be accurately predicted for any load position and for different configurations: single span or multi-span profiles, uphill or downhill yarding, self-motorized or classical carriage. An additional step toward adaptability is to integrate both full and partial suspension of the logs. Currently this work only deals with full suspension which is true only for short logs extraction. However, full tree yarding with branches processing at the landing area becomes more and more frequent. This extraction method implies partial suspension of the log which can change consequently the tensile forces (Tobey 1980). This topic has already been investigated, especially in North America (Falk 1981; Kendrick and Sessions 1991). Integrating a module able to take into accounts both full and partial suspension suggests also to cross our model with a high definition DTM in order to consider the interaction between the logs and the ground. Currently the model only considers a maximum skyline tensile force in order to ensure safety of operator. It could also be interesting to consider a minimum skyline tensile force which could be required to allow the passage of the loaded carriage over intermediate supports.

The field experiments conducted within this study showed the applicability of our model to real cable yarding operations. The results from this field data acquisition could be a first step toward an international database on cable yarding operations. However such field acquisitions are expensive and require very specific material. Future field acquisitions have to be chosen carefully in order to cover a wide range of situations. In addition to load path and tensile forces, further experimental measurements could concern friction at the intermediate supports and tension variation caused by partial suspension of the logs. Our experience during the real experiment showed that the use of load cell restricts the location of the skyline tensile force measurement. In further field experiments, portable wire rope tensiometers could be advantageously used to be free to measure the tensile force anywhere along the skyline.

At last, the real cable yarding operation followed in this study represents a typical operation in the Alps (uphill yarding with a short line on steep slope). However, in order to complete the validation of the model, further follow ups of cable operation could be done to test the accuracy in other configurations. The final validation could lead to an automatic optimization of cable yarding operations able to propose a solution for initial tensioning and intermediate support positioning. The calculation time observed for modeling the real experiment varied from 0.8 ms (basic calculation) to 0.5 s (mainline and friction integrated to the model) which is efficient enough for this kind of adaptation.

Acknowledgments

This study has been carried out within the framework of the Interreg - Alpine Space Programme during the project Newfor n° 2-3-2-FR: “New technologies for a better mountain forest timber mobilization”. Website: www.newfor.net

References

Akay AE, Oğuz H, Karas IR, Aruga K (2008) Using LiDAR technology in forestry activities. Environ Monit Assess 151:117–125

Auban J-M, Bartoli M (1997) Forest roads in mountainous regions - Assessment and technical proposals. An example in the central Pyrenees. Rev For Fr 49:235–246

Bartoli M (2007) "Lombardi in Arudy!". A snapshot of logging in the French Pyrenees from 1916 to 1975. Rev For Fr 59:85–92

Bartoli M (2008) Dossier débardage par câble. For. Fr. 511:20–22

Bont L, Heinimann HR (2012) Optimum geometric layout of a single cable road. Eur J For Res 131:1439–1448

Brändli U-B (2010) Inventaire forestier national suisse. Résultats du troisième inventaire 2004–2006. Birmensdorf, Institut fédéral de recherches sur la forêt, la neige et le paysage WSL, Berne, Office fédéral de l'environnement

Carson WW (1977) Analysis of the Single Cable Segment. For Sci 23:238–252

Carson WW, Studier DD, Lysons HH (1971) Running skyline design with a desk-top computer-plotter. Pacific North West Forest and Range Experiment Station, Forest Service, U.S. Dept. of Agriculture

Cavalli R (2012) Prospects of Research on Cable Logging in Forest Engineering Community. Croat J For Eng 33:339–356

Charland J, Hernried A, Pyles M (1994) Cable Systems with Elastic Supporting Elements. J Struct Eng 120:3649–3665

Chung J (1987) Development of a cable logging system analysis package for micro-computers. Report of the Oregon State University

Chung W (2002) Optimization of cable logging layout using a heuristic algorithm for network programming. Thesis, Oregon State University, USA

Chung W, Sessions J (2003) A computerized method for determining cable logging feasibility using a DEM. In: "Forest Operations Among Competing Forest Uses". COFE 2003, Proceedings of the Council on Forest Engineering (COFE), Bar Harbor, ME, USA, 7-10 October 2003

Fabiano F, Marchi E, Neri F, Piegai F (2011) Skyline tension analysis in yarding operation: case studies in Italy. In: Pushing the boundaries with research and innovation in forest engineering. FORMEC 2011, Proceedings of the 44th International Symposium on Forestry Mechanisation, Graz, Austria, 9-13 October 2011. Institute of Forest Engineering, University of Natural Resources and Life Sciences, Graz, Austria

Falk GD (1981) Predicting the payload capability of cable logging systems including the effect of partial suspension. USDA Forest Service Research, Broomall

Grulois S (2013) Les systèmes d'exploitation forestière dans les Alpes françaises. In: Newfor French mid-term Conference, Grenoble 24 October 2013.

Hollaus M, Wagner W, Eberhöfer C, Karel W (2006) Accuracy of large-scale canopy heights derived from LiDAR data under operational constraints in a complex alpine environment. ISPRS J Photogramm Remote Sens 60:323–338

Hunter JD (2007) Matplotlib: A 2D Graphics Environment. Comput Sci Eng 9:90–95.

Irvine HM (1981) Cable Structures. MIT Press, Cambridge, Massachusetts, USA

Kato S (1964) A Note on the KATO-HORI's Tension Formulas for the Calculation of the Skyline Cables. Report of the Tokyo University Forests, 15:14-22

Kendrick D, Sessions J (1991) A solution procedure for calculating the standing skyline load path for partial and full suspension. For Prod J 41:57–60.

Lyons CK (2008) Considering Cable Stretch in Logging Applications. Int J For Eng 19:29–35

McColl IR, Waterhouse RB, Harris SJ, Tsujikawa M (1995) Lubricated fretting wear of a high-strength eutectoid steel rope wire. Wear 185:203–212

Oliphant TE (2007) Python for Scientific Computing. Comput Sci Eng 9:10–20

Pestal E (1961) Seilbahnen und Seilkrane für Holz-und Materialtransport. Georg Fromme & Co, Vienna, Austria

Sessions J (1976) Field measurement of cable tensions for skyline logging systems. Corvallis, Or. : Forest Research Laboratory, School of Forestry, Oregon State University

Tobey AC (1980) Skyline analysis with log drag. Report of the Oregon State University

Vidal C (2010) La Forêt française - Les résultats issus des campagnes d'inventaire 2005 à 2009 - Rhône-Alpes. Inventaire Forestier National, Nogent-sur-Vernisson, France

Ypma T (1995) Historical Development of the Newton–Raphson Method. SIAM Rev 37:531–551

Zweifel O (1960) Seilbahnberechnung bei beidseitig verankerten Tragseilen. Schweiz Bauztg 1:1–4.

The final publication is available at Springer via http://dx.doi.org/10.1007/s10310-015-0503-4

Annex 1 *Description of the general model process (see Table 1 for the description of parameters). First step consists in calculating the skyline unstrained length that corresponds to the initial configuration of the system. Second step is the calculation of load path and tensile forces. If considered, mainline and friction effects are integrated in both step.*

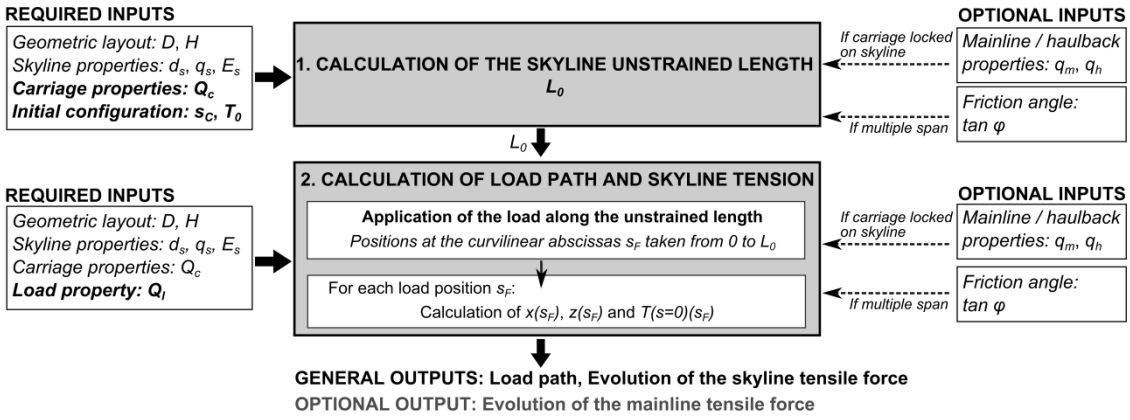

Annex 2 *Scheme of the small scale field experiment for the double span configuration. SPAN 1 was also used for the single span configuration.*

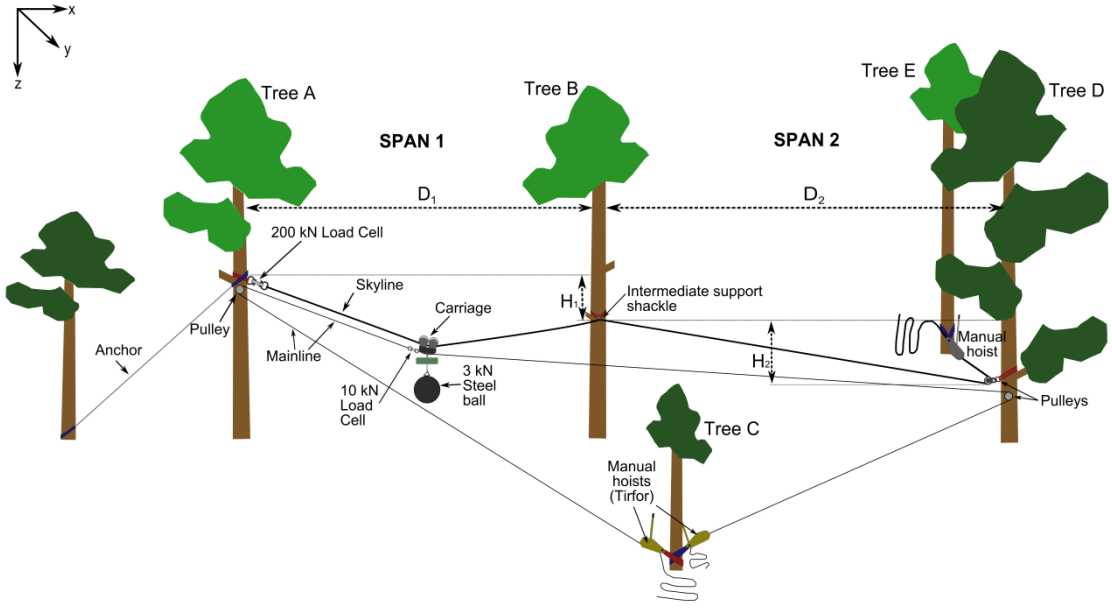

The final publication is available at Springer via http://dx.doi.org/10.1007/s10310-015-0503-4

Annex 3 *Scheme of the real cable yarding operation followed. Measurements concern the situation when the load is located on SPAN 2 to ensure a full suspension of the log.*

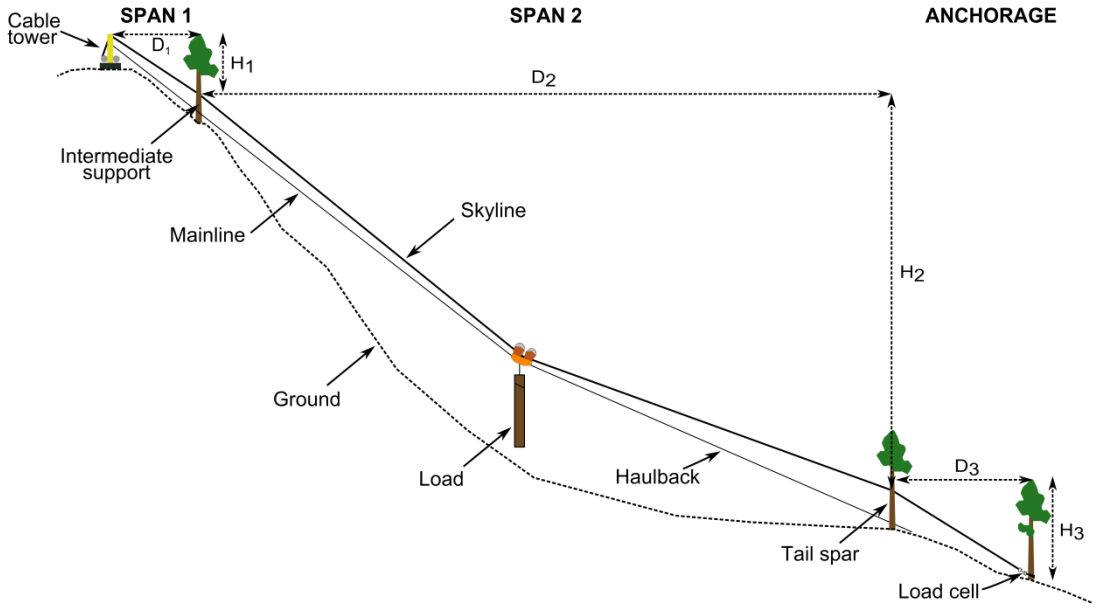

The final publication is available at Springer via http://dx.doi.org/10.1007/s10310-015-0503-4